THERMOANALYTICAL INVESTIGATIONS ON KINETICS AND MECHANISM OF DEAMINATION OF TRIS(ETHYLENEDIAMINE)COPPER(II) SULPHATE

C. G. R. Nair, Suresh Mathew and K. N. Ninan *

DEPARTMENT OF CHEMISTRY, UNIVERSITY OF KERALA, TRIVANDRUM 6950 34, INDIA
*PROPELLANT AND SPECIAL CHEMICALS GROUP, VIKRAM SARABHAI SPACE
CENTRE, TRIVANDRUM 6950 22, INDIA

The thermal decomposition of tris(ethylenediamine)copper(II) sulphate has been studied using TG, DTG and DTA. The different stages of decomposition have been identified by these techniques in conjunction independent pyrolysis and X-ray diffraction. The kinetics and mechanism of the first two stages of deamination of the complex were evaluated. The activation parameters for the deamination reaction were computed from the TG and DTA curves using four integral methods. The two stages of deamination follow the mechanism of random nucleation with the formation of one nucleus on each particle (Mampel equation). The thermodynamic parameter namely heat of reaction (ΔH) for the two deamination processes was also evaluated.

Introduction

The thermal decomposition of transition metal amine complexes in the solid-state has been investigated phenomenologically by several researchers [1–3]. However, a search through the literature revealed that very few attempts have been made to undertake a quantitative study on the kinetics and mechanism of thermal deamination reactions [4–6]. In the present work, both thermogravimetry and differential thermal analysis have been used to evaluate these aspects of deamination reaction.

In our earlier publications, we have reported the kinetics and mechanism of thermal decomposition of complexes containing both monodentate and bidentate ligands [7–9]. In this paper we report the results of our study on the thermal deamination of tris(ethylenediamine)copper(II) sulphate using TG, DTG, DTA and other accessory techniques which have been used for

exploring the kinetic, mechanistic and thermodynamic aspects of these reactions.

Experimental

Preparation of [Cu(en)₃]SO₄

The complex was prepared according to the method of Birdwhistell [10]. The deep blue coloured complex was characterized by spectral and chemical methods. The elemental analysis was carried out using Carlo Erba microelemental analyser. The results of the analysis are given in Table 1.

Table 1 Analytical result for [Cu(en)₃]SO₄

	Theoretical %	Observed %
Copper	18.71	18.57
Carbon	21.20	21.06
Hydrogen	7.06	7.12
Nitrogen	24.73	24.24

Instruments

The TG-DTG and DTA curves were recorded using a DuPont model 2000 Thermal Analyst in conjunction with 951 thermogravimetric analyser and 1200 DTA cell using a platinum crucible. The experiments were carried out in pure nitrogen atmosphere at a flow rate of 50 $cm^3 min^{-1}$. The heating rate employed was 10 $deg \cdot min^{-1}$ and sample mass 10 mg. The area under the DTA curve was evaluated by the sigmoidal curve integration using the Thermal Analysis Soft Ware, and the calibration was done using pure indium (for I stage) and lead (for II and III stages) for enthalpy measurement. The X-ray powder diffractograms were recorded using a Philips 1710 diffractometer with a PW1729 X-ray generator using CuK_α radiation. Computational work was done with an IBM-PC/XT using FORTRAN 77 program.

Results and discussion

The TG-DTG-DTA curves for tris(ethylenediamine)copper(II) sulphate are shown in Fig. 1. The temperature of inception (T_i), completion (T_f) and
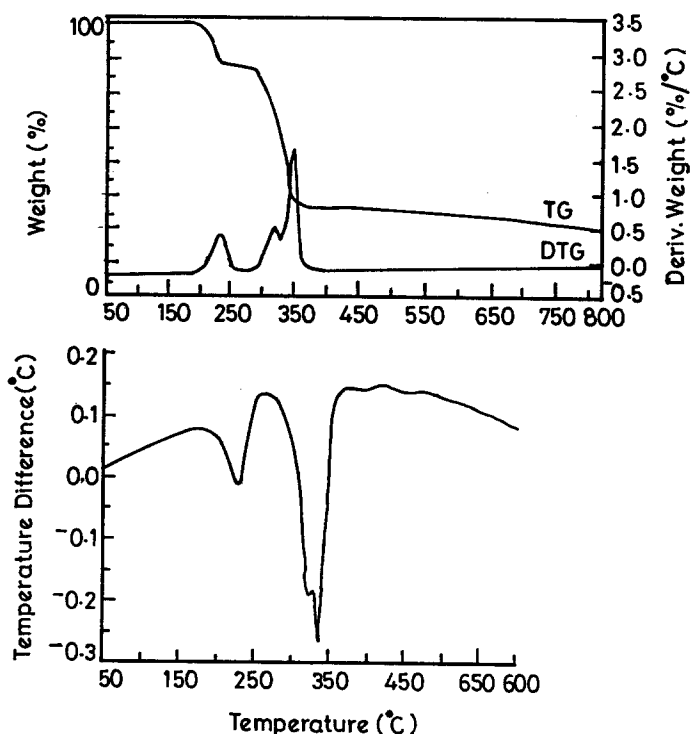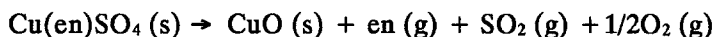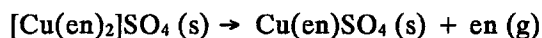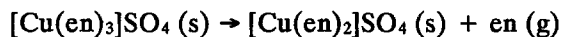
Fig. 1 TG

peak (T_s for DTG and T_p for DTA) for each stage of decomposition are given in Table 2. The results obtained from independent pyrolysis agree well with the TG data. The weight loss data show that tris(ethylenediamine)copper(II) sulphate decomposes in three stages as follows:

$$[Cu(en)_3]SO_4 \text{ (s)} \rightarrow [Cu(en)_2]SO_4 \text{ (s)} + en \text{ (g)}$$

$$[Cu(en)_2]SO_4 \text{ (s)} \rightarrow Cu(en)SO_4 \text{ (s)} + en \text{ (g)}$$

$$Cu(en)SO_4 \text{ (s)} \rightarrow CuO \text{ (s)} + en \text{ (g)} + SO_2 \text{ (g)} + 1/2O_2 \text{ (g)}$$

The first mass loss ($T_s = 230°C$) corresponds to the loss of one ethylenediamine (en) molecule to form stable $[Cu(en)_2]SO_4$. This compound could be a square planar product formed by the decomposition of the tris(ethylenediamine)copper(II) sulphate having octahedral geometry. Usually in bis(ethylenediamine) complex, the copper(II) ion will occupy essentially a tetragonal environment, with the ethylenediamine ligands coor-

dinating to form a square coplanar structure with the methylene groups of the ligand occupying a gauche configuration [11]. The second stage corresponds to the deamination of the bis(ethylenediamine) complex to form the unstable intermediate $Cu(en)SO_4$. However, from DTG and DTA curves, this deamination stage seems to be overlapping with the subsequent reaction. The formation of the mono(amine) complex has been reported in an earlier publication [8]. Since copper(II) usually has a coordination number four, this product could be formed by an anation reaction [12]. The third stage corresponds to the decomposition of $Cu(en)SO_4$ to form a mixture of CuO and $CuSO_4$, which gets ultimately converted to CuO. The weight loss from 400–800°C is a slow process for which well-defined DTG and DTA peaks could not be obtained.

Table 2 Phenomenological data for the thermal decomposition of [Cu(en)3]SO4

Stages	I	II	III	IV
Decomposition mode	Loss of one en	Loss of one en	Decomposition of Cu(en)2SO4 to xCuSO4·yCuO	Decomposition to CuO
TG results				
T_i	185	275	325	375
T_f	250	325	375	800
T_s	230	313	342	–
% wt. loss				
Theoretical	17.67	17.67	41.23	
Observed	17.5	17.5	32.5	8.8
Independent pyrolysis				
Theoretical				76.57
Observed				75.63
Residue				CuO
DTA				
T_i	190	278	333	375
T_f	253	333	367	600
T_p	232	325	337	–
ΔH (cal·g^{-1})	48	162		–

The heat of reaction (ΔH) calculated from DTA curves for the first stage of deamination is 48 cal·g^{-1}, whereas the overall heat of reaction for the second and third stage is 162 cal·g^{-1}. The higher value in enthalpy is

ascribable to the additive effect of both the deamination and the decomposition reactions.

Table 3 X-ray powder diffraction data

[Cu(en)₃]SO₄		[Cu(en)₂]SO₄		$CuO \cdot CuSO_4$		CuO	
$d(Å)$	I/I_o	$d(Å)$	I/I_o	$d(Å)$	I/I_o	$d(Å)$	I/I_o
3.8939	100.00	7.4206	100.0	2.5372	100.0	2.338	100.0
4.5181	79.24	5.0230	27.04	2.3324	92.51	2.5444	86.57
3.2889	37.80	4.0687	20.64	1.8695	48.80	1.8722	42.28
4.8282	34.19	4.7032	15.41	1.5856	43.11	1.5102	35.78
3.6166	29.13	3.2269	11.29	1.7146	37.42	1.3801	35.23
2.8253	20.14	3.6928	7.81	3.8606	37.12	1.4164	31.65
2.0402	18.43	2.9500	7.78	4.5730	36.22	1.5877	30.74
3.0380	16.75	2.6664	5.74	2.1323	35.02	1.2661	27.59
1.6882	15.69	2.7599	5.34	2.7752	33.53	1.3077	26.41
6.0743	13.53	3.5245	5.16			1.7168	26.10
2.1687	12.47	2.5164	5.03			1.0922	24.92
2.1126	12.37	2.0339	4.73			1.1693	24.76
1.5936	11.50	1.8535	4.69			1.1586	24.13
7.1751	11.47	2.2587	4.45			2.7752	23.81
2.6036	9.15	1.7171	4.39			1.1968	23.11
1.7533	9.15	1.7555	4.05			1.0742	22.83
2.5072	8.92	2.0781	4.05			1.1248	22.16
2.2064	8.08	1.7945	3.96			1.5592	20.78
1.8635	7.66	2.1712	3.89			1.9649	20.74
4.0930	6.99	3.0944	3.77			2.1396	20.70
1.7865	6.54	6.0758	3.70			2.0474	19.60
1.6372	6.54	1.9672	3.60			1.7814	19.37
1.8012	6.47	1.9174	3.57			2.7047	19.37
1.9572	5.54	2.3146	3.45			3.6255	18.66
		2.4360	3.45			3.4420	18.11

The X-ray powder diffraction studies were carried out with the two intermediates isolated by keeping the complex in a programmable muffle furnace at 275° and 400°C respectively as well as the final residue obtained at 800°C under identical conditions. The major intensities along with the d spacings are given in Table 3. The XRD data revealed that the residue separated at 400°C is a mixture of CuO-CuSO₄. The existence of the oxysulphate phase is reported by Brittain et al. [13]. A comparison of the powder diffractograms

with the JCPDS powder diffraction file has shown that the final residue (800°) obtained is CuO [14]. The percentage mass loss for the four stages obtained from the TG curve conforms with the above scheme of reaction.

Kinetics and mechanism

Kinetic and mechanistic studies were done only for the first two stages of deamination since the third stage of deamination is superimposed by the decomposition of $CuSO_4$. Since the second and third stages of decomposition are not separated in DTA, the kinetic analysis was attempted only for the first stage peak. The final process in the decomposition took place as an indistinct step over a long range of temperature, hence no kinetic parameters could be evaluated for the reaction.

Table 4 Kinetic parameters for the deamination of tris(ethylenediamine)copper(II) sulphate using non-mechanistic equations from TG and DTA

		TG		DTA
		Stage I	Stage II	Stage I
n		1.47	1.31	1.47
	CR	203.13	330.08	222.82
E	MT	204.32	333.65	224.16
$(kJ \cdot mol^{-1})$	HM	218.08	346.93	240.52
	MKN	203.23	330.09	222.90
	CR	3.17×10^{19}	6.30×10^{27}	3.51×10^{21}
A	MT	3.93×10^{19}	1.72×10^{28}	4.65×10^{21}
(s^{-1})	HM	1.14×10^{21}	2.04×10^{29}	2.43×10^{23}
	MKN	3.27×10^{19}	6.39×10^{27}	3.60×10^{21}
	CR	0.9990	0.9997	0.9983
r	MT	0.9991	0.9997	0.9984
	HM	0.9987	0.9995	0.9989
	MKN	0.9990	0.9997	0.9983

CR – Coats-Redfern, MT – MacCallum-Tanner, HM – Horowitz-Metzger, MKN – Madhusudanan-Krishnan-Ninan

The kinetic parameters were calculated from the TG and also from DTA curves using four non-mechanistic equations, viz. Coats-Redfern [15], Mac-Callum-Tanner [16], Horowitz-Metzger [17] and Madhusudanan-Krishnan-Ninan [18]. The order parameters, '*n*' were evaluated using a computer by an iterative check on the linearity of Coats-Redfern plots constructed from

TG data by varying n in the range of 0 to 2 in increments of 0.01. The value of n giving the best linear plot was chosen as the order parameter.

The data using the non-mechanistic equations from TG and DTA are given in Table 4. The correlation coefficients (r) are in the range 0.9983–0.9997 indicating nearly perfect fits. It can be seen from this table that the order parameter for the deamination process is a fraction. It is known from the literature [19–20] that this apparent order, n does not necessarily have to be an integer.

Table 4 shows that the activation parameters computed with Horowitz-Metzger equation are higher than the values from the other three equations. This is due to the inherent error involved in the approximation method employed in the derivation of Horowitz-Metzger equation. The higher values of activation energy from DTA technique may be due to the lag in the measurements of temperature as compared to mass measurements. Similar observations has been made by several authors [21–22].

Choice of reaction mechanism

Deduction of the mechanism using the rate equation

$$\mathrm{d}(\alpha)/\mathrm{d}T = A/\varphi e^{-E/RT} f(\alpha)$$

has been discussed by Šestak and Berggren [23]. The mechanism-non-invoking equations have been derived by assuming $f(\alpha) = (1-\alpha)^n$ as in homogeneous kinetics. In contrast, in mechanism-invoking methods, various forms are assumed for $f(\alpha)$ depending on the proposed reaction mechanism and the mechanism is obtained from the $f(\alpha)$ that gives the best representation of the experimental data. In this study, the nine mechanistic models recommended by Šatava [24] were used for curve-fitting the TG and DTA data. The Coats-Redfern method was used for solving the exponential integral, as it is one of the best approaches recommended by several authors [25–27]. E and A were calculated in each case from the slope and intercept, respectively.

The values of E and A obtained for the nine mechanistic equations along with the correlation coefficients (r) for the kinetic plots from the TG and DTA data are presented in Table 5. It can be seen that the highest value of correlation coefficients obtained from the two thermal techniques for the two deamination processes are for the Mampel equation (Eq. 5).

Since a few other models also give high correlation coefficients, it is difficult to choose the correct reaction mechanism using the data given in

Table 5 Kinetic parameters for the deamination of tris(ethylenediamine)copper(II)sulphate using mechanistic equations from TG and DTA

Mechanistic			TG		DTA
Eq. No.	Form of $g(\alpha)$		Stage I	Stage II	Stage I
1.	α^2	E	247.15	443.49	279.07
		A	2.97×10^{23}	2.73×10^{37}	5.88×10^{26}
		r	0.97111	0.98278	0.97481
2.	$\alpha + (1-\alpha)\ln(1\alpha)$	E	273.62	487.30	305.88
		A	1.29×10^{26}	1.65×10^{41}	2.71×10^{29}
		r	0.98065	0.98938	0.98402
3.	$[1-(1-\alpha)^{1/3}]^2$	E	309.22	543.88	342.63
		A	2.47×10^{29}	6.70×10^{45}	6.70×10^{32}
		r	0.99021	0.99537	0.99329
4.	$(1-2/3\alpha) - (1-\alpha)^{2/3}$	E	285.23	505.89	317.81
		A	5.52×10^{26}	1.97×10^{42}	1.24×10^{30}
		r	0.98432	0.99181	0.98764
5.	$-\ln(1-\alpha)$	E	170.23	297.89	187.83
		A	7.04×10^{15}	6.22×10^{24}	4.74×10^{17}
		r	0.99539	0.99854	0.99821
6.	$[-\ln(1-\alpha)]^{1/2}$	E	80.99	144.14	89.80
		A	1.88×10^6	6.25×10^{10}	1.61×10^7
		r	0.99539	0.99854	0.98801
7.	$[-\ln(1-\alpha)]^{1/3}$	E	51.25	92.89	57.13
		A	1.03×10^3	1.14×10^6	4.45×10^3
		r	0.99485	0.99839	0.99791
8.	$1 - (1-\alpha)^{1/2}$	E	141.73	253.20	158.14
		A	2.31×10^{12}	2.03×10^{20}	1.19×10^{14}
		r	0.98536	0.99264	0.98889
9.	$1 - (1-\alpha)^{1/3}$	E	150.50	267.13	167.20
		A	1.48×10^{13}	2.74×10^{21}	8.09×10^{14}
		r	0.98966	0.99524	0.99292

$E / \text{kJ mol}^{-1}; A / \text{s}^{-1}$

Table 5 alone. In such cases the operating mechanism can also be chosen by comparing the kinetic parameters with those obtained by non-mechanistic equation [28]. In the present case a comparison with the values obtained by the Coats-Redfern method will be more appropriate as the same method was used for solving the exponential integral. The good agreement between values of kinetic parameters calculated using Coats-Redfern method and Mampel equation for both TG and DTA indicate that the rate controlling

process for the deamination reaction is random nucleation with one nucleus on each particle.

*   *   *

References

1 W. W. Wendlant and J. P. Smith, The Thermal Properties of Transition Metal Ammine Complexes, Elsevier, Amsterdam, 1967.
2 T. Sato, T. Suda, H. Uchida and T. Okabe, Bull. Chem. Soc. Jpn, 51 (1978) 2310.
3 C. De, P. K. Biawas and N. R. Chaudhuri, Bull. Chem. Soc. Jpn, 56 (1983) 3145.
4 C. G. R. Nair and K. N. Ninan, Thermochim. Acta, 23 (1978) 161.
5 C. G. R. Nair, S. Mathew and K. N. Ninan, Proc. 7th National Symposium on Thermal Analysis, Srinagar, 1989. p. 78.
6 K. Nagase and T. Tanaka, Bull. Chem. Soc. Jpn, 46 (1973) 2435.
7 S. Mathew, C. G. R. Nair and K. N. Ninan, Thermochim. Acta, 144 (1989) 33.
8 C. G. R. Nair, S. Mathew and K. N. Ninan, Thermochim. Acta, 150 (1989) 63.
9 S. Mathew, C. G. R. Nair and K. N. Ninan, Bull. Chem. Soc. Jpn., 64 (1991) in press.
10 G. Gordon and R. K. Birdwhistell, J. Amer. Chem. Soc, 81 (1959) 3567.
11 I. M. Procter, B. J. Hathaway, and P. Nicholls, J. Chem. Soc. (A) (1968) 1678.
12 J. E. House, Jr. and F. M. Tahir, Thermochim. Acta, 118 (1987) 191.
13 R. D. Brittain, K. H. Lau and D. L. Hilbenbrand, J. Phys. Chem. 93 (1989) 5316.
14 Hannewalt Method Search Manuel, International Centre for Diffraction Data, JCPDS, Swarthmore, PA, p. 748.
15 A. W. Coats and J. P. Redfern, Nature, 201 (1964) 68.
16 J. R. MacCallum and J. Tanner, Eur. Polym. J., 6 (1970) 1033
17 H. H. Horowitz and G. Metzger, Anal. Chem., 35 (1963) 1464
18 P. M. Madusudanan, K. Krishnan and K. N. Ninan, Thermochim. Acta, 97 (1986) 189.
19 D. Blecic and Z. D. Zivkovic, Thermochim. Acta, 60 (1983) 68.
20 A. C. Norris, M. I. Pope and M. Selwood, Thermochim. Acta, 41 (1980) 357.
21 E. F. Palermo and J. Chiu, Thermochim. Acta, 14 (1976) 1.
22 P. M. Madhusudanan, K. Krishnan and K. N. Ninan, Proc. 3rd National Symposium on Thermal Analysis, Trivandrum, 1981. p. 46.
23 J. Šestak and G. Berggren, Thermochim. Acta, 3 (1971) 1.
24 V. Šatava, Thermochim. Acta, 2 (1971) 423.
25 M. D. Judd and M. I. Pope, J. Thermal Anal., 4 (1972) 31.
26 J. Zsako, J. Thermal Anal., 5 (1973) 239.
27 V. M. Gorbachev, J. Thermal Anal., 8 (1975) 349.
28 P. H. Fong and D. T. Chen, Thermochim. Acta, 18 (1977) 273.

Zusammenfassung — Mittels TG, DTG und DTA wurde die thermische Zersetzung von Tris(ethylendiamin)-kupfer(II)-sulfat untersucht. Anhand dieser Methoden wurden in Verbindung mit einer gesonderten Pyrolyse und Röntgendiffraktion die einzelnen Schritte dieser Zersetzung identifiziert. Weiterhin wurde die Kinetik und der Mechanismus der beiden

ersten Schritte der Desaminierung des Komplexes entwickelt. Unter Anwendung von vier Integralmethoden wurden aus den TG- und DTA-Kurven die Aktivierungsparameter der Desaminierungsreaktion berechnet. Beide Schritte der Desaminierung verlaufen nach dem Mechanismus der Random-Keimbildung mit der Bildung von einem Keim pro Partikel (Mampel-Gleichung). Die Reaktionswärme der zwei Desaminierungsprozesse wurde ebenfalls bestimmt.